J Mater Sci (2022) 57:12985–12993

Materials for life sciences

Biological investigation of chromium-doped cobalt oxide nanoparticles against HeLa cancer cell lines

Sivaranjani Sivalingam[1], Vijaykumar Murugan[1], and P. P. Vijaya[1,*]

[1] *Department of Nanoscience and Technology, Bharathiar University, Coimbatore 641046, India*

Received: 16 December 2021
Accepted: 10 June 2022
Published online: 5 July 2022

ABSTRACT

Cobalt oxide nanoparticles have a lot of usage in cancer nanomedicine due to their wide variety of biological uses. Varied concentrations of chromium-doped cobalt oxide (1%, 3%, 5% Cr: Co_3O_4) nanoparticles and cobalt oxide (Co_3O_4) nanoparticles were synthesized using the co-precipitation method and characterized and confirmed by XRD, FESEM, EDS and FTIR methods. The nanoparticles were then used to assess DNA damage using the hemolysis and comet assay. In addition, the cell viability assessments were carried out on HeLa cervical cancer cell lines. The outcomes suggest that the prepared nanoparticles were highly hemocompatible, showing inducible DNA damage via tail moments. The cell viability assays showed that the nanoparticles have detrimental effects on the cancer cells via morphological and MTT assay results. Therefore, the studied concentrations of Cr-doped Co_3O_4 can be further used as an efficient hemocompatible and anti-cancer-based nanomaterial in future therapeutic aspects.

Introduction

Cancer is a deadly and diverse collection of diseases produced by a sequence of clonally selected mutations in critical tumor-suppressor genes and oncogenes with varying biological characteristics. It is described as the uncontrollable division of aberrant cells or tissues with the capacity to invade and destroy normal bodily tissue [1]. Cancer nanomedicine is a field of bio-nanotechnology that is still developing, having a crucial function in the treatment of cancer advanced treatment ideas and methods [2]. Biocompatibility has long been regarded as one of the essential factors invalidating a biomaterial for use in human organisms. Biocompatibility can be assessed using "in vivo" and "in vitro" tests. The comet assay, also known as single-cell gel electrophoresis (SCGE), is a popular technique used to measure and analyze DNA breakage in individual cells that can be used in in vitro, ex vivo and in vivo systems [3]. The comet assay is a valuable tool for analyzing oxidative stress issues in human lymphocytes. The use of specific antioxidants has allowed for the elucidation of the

Handling Editor: Christopher Blanford.

Address correspondence to E-mail: vijayaparthasarathy@buc.edu.in

https://doi.org/10.1007/s10853-022-07432-0

mechanism of DNA damage due to the wide range of agents. Additionally, the comet assay revealed the pro-oxidant/antioxidant effects of various endogenous and exogenous compounds. Metabolic cell viability assays were done using tetrazolium salts like MTT and are mainly used for the screening of anticancer activity of compounds on cultured cells [4].

Chemical techniques, thermal breakdown, electrochemical processes, microwave irradiation, and laser ablation have all been used to create metallic nanoparticles. Metal oxide nanoparticles are critical developments in research because of their wide range of medical and biotechnological applications in drug delivery systems, biosensing, cancer therapy, advanced biomedical purpose and cell imaging [5]. Cobalt is one of the significant elements in metal biomedical application, and its metal oxide-based research has an interest in the preparation of nanoparticles for various biomedical applications such as anti-cancer, antibacterial, enzyme inhibition properties and antifungal [6, 7]. Currently, Co_3O_4 nanoparticles are some of the p-type semiconducting material with spinel structure having high mechanical strength and chemical stability at high temperatures. The spinel structures of Co_3O_4 exhibit a cubic closed packing array of oxide ions, in which Co^{2+} ions occupy the 1/8 tetrahedral A sites and Co^{3+} ions occupy 1/2 octahedral B sites [8]. The nanoparticles of transition metal oxides are also being widely used in developing anode materials for rechargeable Li batteries, catalysis, magnetic materials, pigments, gas sensor, high-temperature solar selective absorbers and photocatalysts [9, 10]. Co_3O_4 nanoparticles are also a promising visible light photocatalysis due to their high surface area, high chemical reactivity and favorable bandgap (1.7–2.4 eV) in this field. They are used to absorb photons in the visible range [11].

The metal oxide efficiency of Co_3O_4 nanoparticles can be improved by increasing the surface defects such as doping transitions that lead to higher biological activities and free radicals produced in an oxidation reaction [12, 13]. Doping of chromium (Cr) has various oxidation states, a valuable component of metalloproteins and enzymes. Cr doping in Co_3O_4 nanoparticles has received a lot of attention in biomedical applications because it can improve the biocompatibility response by reducing the toxicity of the nanoparticles [14]. Several methods are used for the synthesis of Cr-doped Co_3O_4 nanoparticles, and they include mechanochemical, soft chemical, microemulsion, chemical, sol–gel and co-precipitation methods, in which co-precipitation technique is a simple process used to control the size of nanoparticle synthesized [15].

In the current study, we describe that the Co_3O_4 nanoparticles are one of the most unique and attractive materials in biomedical research based on their bioactivity. The toxicity (or) biocompatibility of Co_3O_4 nanoparticles and Cr-doped Co_3O_4 nanoparticles were analyzed by confirming the DNA damage and reduced cell viability mechanisms seen in comet and MTT assays, respectively.

Materials and methods

Materials

Cobalt chloride hexahydrate ($CoCl_2{\cdot}6H_2O$), chromium chloride hexahydrate ($CrCl_2{\cdot}6H_2O$) and ammonia solution were purchased from Sigma-Aldrich and HiMedia and used without further purification. Double distilled water (DDW) was used throughout the research.

Synthesis of cobalt oxide nanoparticles

The Co_3O_4 nanoparticles were synthesized using the co-precipitation method. The experiment typically consisted of 0.1 M cobalt chloride hexahydrate dissolved in 50 mL of distilled water and stirred for 30 min. $NH_3{\cdot}H_2O$ (25%) solution was added to the above mixture under continuous stirring at room temperature until pH 11 was attained. After stirring, the reaction mixture was refluxed at 180 °C for 2 h. The product was aged for 24 h, resulting in a residue that was centrifuged at repeated washing steps using distilled water to obtain the final product dried at 80 °C at least for 2 h, and the as-obtained sample was further annealed at 400 °C for 3 h [8, 15].

Synthesis of chromium-doped cobalt oxide nanoparticles

In the preparation process, the addition of cobalt precursors at different percentages of Cr (1, 3 and 5%) concentrations to form Cr-doped Co_3O_4 is crucial for preparing the test samples. The $NH_3{\cdot}H_2O$ (25%) solution was then added to the above-prepared solutions of different concentrations under

continuous stirring until the pH11 was attained at room temperature for 30 min. This reaction mixture was then refluxed at 180 °C for 2 h. The end product was aged for 24 h, resulting in a concentrated precipitate that was centrifuged, followed by repeated washing with distilled water and annealed at 400 °C for 3 h [16].

In vitro hemocompatibility

In vitro hemocompatibility test was analyzed for both synthesized Co_3O_4 and Cr: Co_3O_4 nanoparticle samples by comparative hemolysis test. In order to do that, the amount of hemoglobin released into the supernatant was determined spectrophotometrically at 540 nm wavelength. The test run consisted of PBS as a negative control and distilled water as a positive control under mixing both solutions with blood making a final concentration of 200 µg/mL. To calculate the rate of hemolysis exerted by the pure Co_3O_4 and Cr: Co_3O_4, the following formula was used [17].

Comet assay

The synthesized pure Co_3O_4 and Cr-doped Co_3O_4 nanoparticles nanocomposite's effect on human leucocyte DNA was assessed using comet assay by Lu et al.'s (2017) method. Alternatively, the level of DNA damage was viewed under the gel documentation system instead of fluorescence imaging. Co_3O_4 was chosen as the reference, and three different concentrations of Cr-doped Co_3O_4 nanoparticle samples (1%, 3% and 5%) were treated on isolated leucocyte genomic DNA that was isolated using the Qiagen DNA isolation kit method (Qiagen Pvt. Ltd., India). Three different volume concentrations of each test sample (Co_3O_4) as 50 µl and 150 µl diluted up to 200 µl using DEPC treated water were tested on 250 µl of 100 ng genomic DNA sample. Based on the recorded results of the comet assay, the DNA damage was measured from the comet head and tail length [18].

Cell culture

The HeLa cells (human cervical cancer cells) were cultured individually in liquid medium (DMEM) supplemented with 10% fetal bovine serum (FBS), 100 µg/ml penicillin and 100 µg/ml streptomycin and maintained under an atmosphere of 5% CO_2 at 37 °C. All cell line was purchased from the National Centre for Cell Sciences (Pune, India).

MTT assay

The various concentrations of test samples of pure Co_3O_4 and Cr-doped Co_3O_4 nanoparticles nanocomposites were analyzed for in vitro cytotoxicity on HeLa cell lines using 3-(4, 5-dimethylthiazol2-yl)-2, 5-diphenyltetrazolium bromide (MTT) assay. The cultured cells were then harvested by the trypsinization method and combined following a 15-ml tube. The cells were then plated at a density of 1 × 105 cells/ml cells/well (200 µL) into a 96-well tissue culture plate in DMEM medium containing 10% FBS and 1% antibiotic liquid for 24–48 h at 37 °C; wells were wiped with sterile PBS and treated with different concentrations of the test sample pure Co_3O_4 and Cr-doped Co_3O_4 nanoparticles nanocomposites in a serum-free DMEM medium.

Each sample was then replicated three times and incubated at 37 °C in a humidified 5% CO_2 incubator for 24 h. Subsequently, during the mentioned incubation period, MTT (20 µL of 5 mg/ml) was added to every well, incubated for 2–4 h, respectively, until purple precipitates were observable under an inverted microscope. The resulting medium combined with MTT (220 µL) was isolated from the wells and washed with 1 × PBS (200 µl). In the method to dissolve formazan crystals, DMSO (100 µL) was added and shaken well for 5 min, after which the absorbance of every sample containing wells was evaluated at 570 nm using a microplate reader (Thermo Fisher Scientific, USA), and the percentage of cell viability and IC50 value was analyzed after tabulating in worksheets [19].

Characterization techniques

The Co_3O_4 and Cr-doped Co_3O_4 samples were characterized using the following techniques. The crystalline structure of the samples was determined by using Rigaku Smart Lab X-ray Diffractometer (XRD) with Cu Ka radiation (1.5406 Å). Morphological analysis was determined by FESEM-EDS (quanta-250-FEG). The hemolysis assay of the nanoparticles was determined by the UV–Vis spectroscopic method (JoscoV-650, Japan).

Results and discussion

XRD analysis

The crystal structure and phase purity of the prepared Co_3O_4 and Cr-doped Co_3O_4 nanoparticles were studied using XRD analysis, as shown in Fig. 1. They depict XRD patterns of Co_3O_4 and Cr-doped Co_3O_4 nanoparticles. The primary characteristic peaks were detected at 19.0°, 31.2°, 36.8°, 38.5°, 44.88°, 55.6°, 59.3° and 65.2°, corresponding to (111), (220), (311), (222), (400), (422), (511), (440) crystallographic spinel cubic phase of pure Co_3O_4 NPs and that is matched well with JCPDS card no. [65-3103]. The intensity of Co_3O_4 was reduced due to the doping of Cr, and an additional extra peak was observed for a higher concentration of Cr-doped Co_3O_4. The average grain size of Co_3O_4 was determined from the most substantial peak (311) and calculated to be 21.5 nm. The grain size of Co_3O_4 and Cr-doped Co_3O_4 nanoparticles was estimated using the Debye–Scherrer formula; the calculated values are given in Table 1 [20, 21].

FTIR analysis

To further confirm the formation of nanocomposites, we have performed FTIR absorption spectra for Co_3O_4, 1% Cr: Co_3O_4, 3% Cr: Co_3O_4 and 5% Cr: Co_3O_4 nanoparticles that are in line with the 400–4000 cm^{-1} region as shown in Fig. 2. The absorption spectra of pure Co_3O_4 nanoparticles exhibit two sharp metal oxide peaks indexed at 570 cm^{-1} and 664 cm^{-1}, which corresponds to the Co–O stretching band of Co_3O_4. The band at 1627 cm^{-1} and 3434 cm^{-1} is indicative for O–H stretching vibration of water molecules. The absorption spectrum of Cr-doped Co_3O_4 samples also exhibits strong metal oxide bands positioned at 570 cm^{-1} and 664 cm^{-1}. However, it is observed that with increasing concentration of Cr doping the intensity of absorption peaks decreases, which is evident from 5% Cr-doped sample, thus confirming the formation of Cr-doped Co_3O_4 nanocomposites [22, 23].

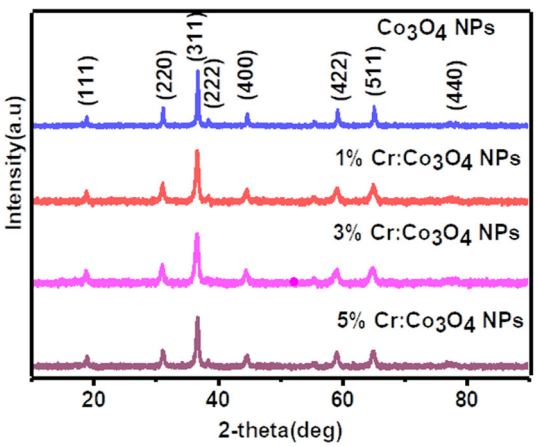

Figure 1 XRD analysis of pure Co_3O_4 nanoparticles and 1, 3 and 5% Cr-doped Co_3O_4 nanoparticles.

Morphological and elemental analysis

Morphological assessments of the prepared nanomaterial were observed by FESEM. As shown in Fig. 3 a confirming the FESEM image of Co_3O_4 nanoparticles and Cr-doped Co_3O_4 nanoparticles at 5 and 2 μm scale magnification, the FESEM image clearly showed an irregular spherical shape with aggregation for pure Co_3O_4 nanoparticles. The change in surface morphology of Cr-doped Co_3O_4 nanoparticles could be due to doping. When the dopant concentration increases, the agglomeration size of the Co_3O_4 nanoparticle also increases [24].

EDS analysis

The energy-dispersive X-ray spectroscopy (EDS) was used to study the elements present in the prepared samples. Figure 4 shows the EDS spectrum of Co_3O_4 nanoparticles and 1%, 3% and 5% Cr-doped Co_3O_4 nanoparticles. The peaks corresponding to Cr were observed in the EDS spectra. The doped samples were confirmed for the presence of a proper proportion of Cr in Co_3O_4 nanoparticles depicting that this can lead to the oxygen deficiency in Co_3O_4 [25].

Table 1 Grain size of Co_3O_4 and Cr-doped Co_3O_4 nanoparticles

Samples	Grain size
CO_3O_4NPS	21.5 nm
1% Cr: Co_3O_4NPS	23.5 nm
3% Cr: Co_3O_4NPS	25.2 nm
%5 Co_3O_4NPS	28.7 nm

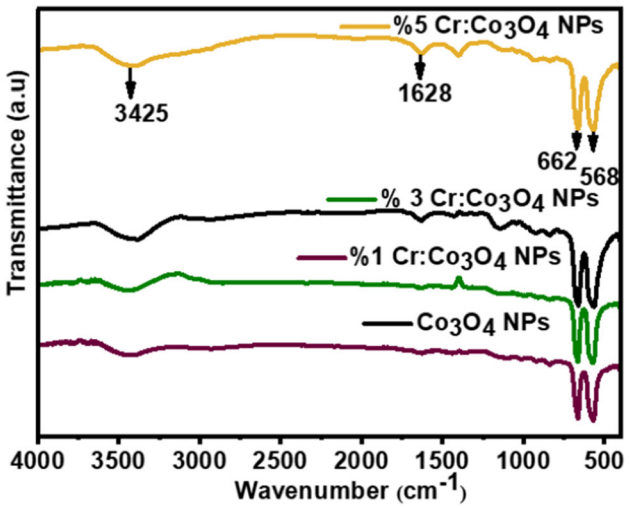

Figure 2 FTIR analysis of pure Co_3O_4 nanoparticles and 1, 3 and 5% Cr-doped Co_3O_4 nanoparticles.

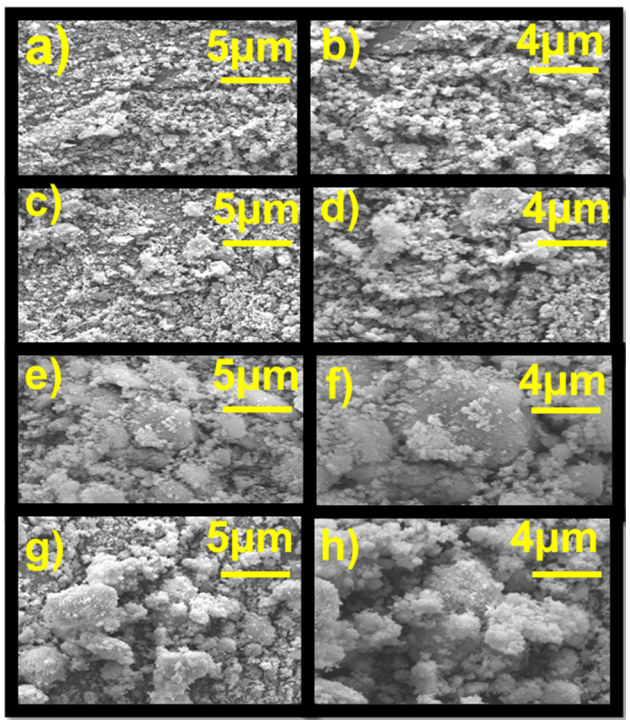

Figure 3 FESEM image of (**a** & **b**) Co_3O_4, (**c** & **d**) 1% Cr-doped Co_3O_4, (**e** & **f**) 3%Cr-doped Co_3O_4 nanoparticles and (**g** & **h**) 5% Cr-doped Co_3O_4 nanoparticles.

In vitro hemocompatibility

The hemolysis assay was performed to test the hemocompatibility of the prepared Co_3O_4 nanoparticle at different concentrations of Cr-doped Co_3O_4 (1, 3 and 5%) on RBC for a range of concentrations (50, 75 and 100 µg/mL) after 3-h incubation. From Fig. 5, it is observed that both Co_3O_4 nanoparticles and that doped with various percentages of Cr exhibited a concentration-dependent increase in the hemolytic activity. Moreover, the obtained hemolytic ratio increased with increasing Cr dopant percentage in Co_3O_4 nanoparticles. Generally, the hemolytic balance is categorized into three levels, 5%, 10%, and > 20% indicating the high hemocompatible, mild hemocompatible, and non-hemocompatible features, respectively. The obtained hemolytic results for pure Co_3O_4, 1% Cr: Co_3O_4, 3% Cr: Co_3O_4 and 5% Cr: Co3O4 nanoparticle at 100 µg/mL concentrations were 3.70, 0.88, 1.45 and 5.70, respectively. Therefore, the observed data confirm that the pure Co_3O_4, 1% Cr: Co_3O_4, 3% Cr: Co_3O_4 show hemolytic ratios less than < 5%. From these results, it is clear that all the prepared samples were highly hemocompatible to human red blood cells at the maximum given concentrations. Interesting, the hemolytic effect of Co_3O_4 nanoparticles was reduced initially when doped with 1% and 3% Cr, although 5% Cr: Co_3O_4 nanoparticles exhibited the highest hemolytic activity than Co_3O_4 nanoparticles, 1% and 3% Cr: Co_3O_4 nanoparticle. This can be attributed to the higher increased concentration of Cr ions released when interacting with RBC membranes and that causes cell membrane disruption, which subsequently releases higher hemoglobin from RBCs. Therefore, the increase in the hemolytic percentage of the Cr: Co_3O_4 nanoparticle is directly proportional to the increased percentage of Cr dopant present in the prepared sample [26, 27].

Elements	Atomic [wt%]
CO	49.39
O	50.61
Total	100.0

Elements	Atomic [wt%]
Co	32.21
O	66.79
Cr	1.01
Total	100.0

Elements	Atomic [wt%]
Co	31.01
O	66.66
Cr	2.32
Total	100.0

Elements	Atomic [wt%]
Co	37.22
O	59.36
Cr	3.42
Total	100.0

Figure 4 EDS analysis of (**a**) Co_3O_4, (**b**) 1% Cr-doped Co_3O_4, (**c**) 3%Cr-doped Co_3O_4, and (**d**) 5%Cr-doped Co_3O_4 nanoparticles.

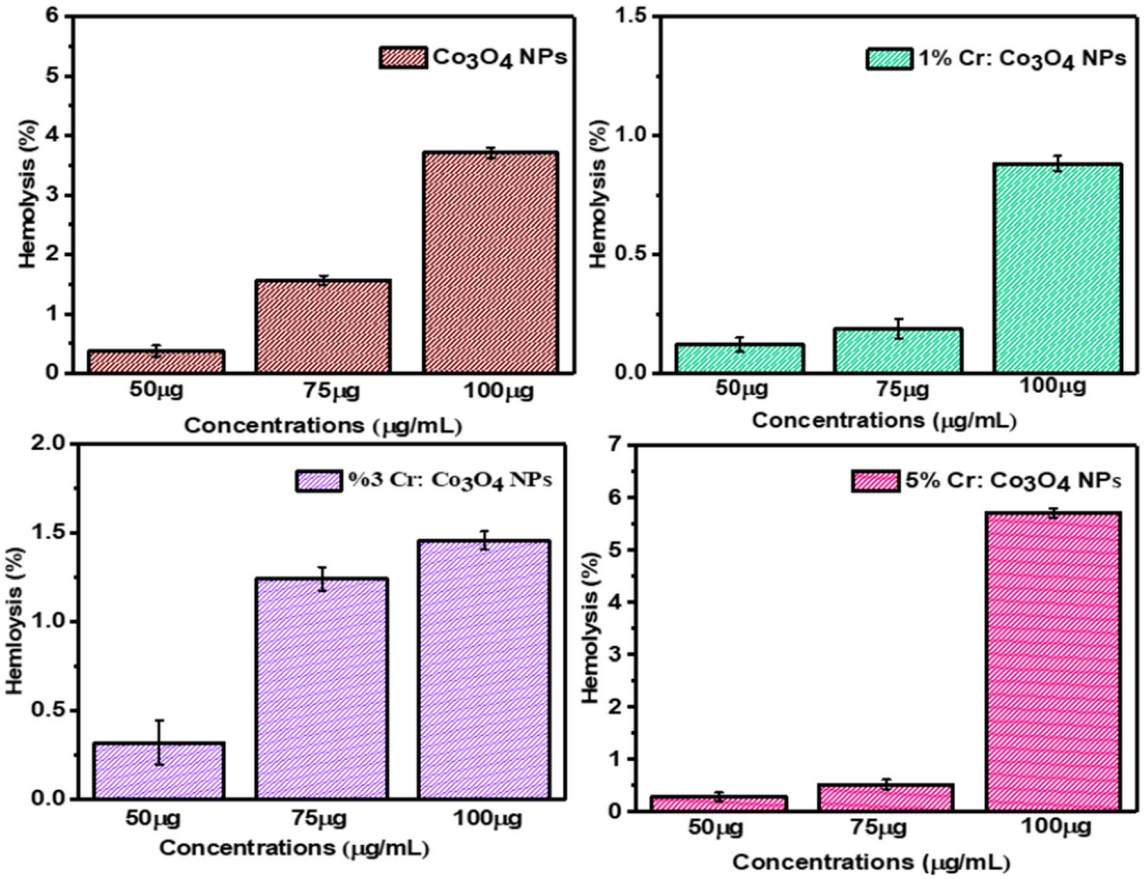

Figure 5 In vitro hemocompatibility study of pure Co_3O_4, 1% Cr-doped Co_3O_4, 3% Cr-doped Co_3O_4 and 5% Cr-doped Co_3O_4 nanoparticles.

Table 2 DNA damage of pure Co_3O_4, 1% Cr: Co_3O_4, 3% Cr: Co_3O_4, and 5% Cr: Co_3O_4 nanoparticles to evaluate the head dia, tail length and comet value in human peripheral blood cells

Concentrations	Co_3O_4NPS	1% Cr: Co_3O_4NPS	3% Cr: Co_3O_4NPS	%5 Co_3O_4NPS
Head Dia	0.5 mm	0.5 mm	0.5 mm	1 mm
Comet value	1.2 mm	0.56 mm	1 mm	0.84 mm

Comet assay

The recorded gel documentation images were measured for the tail and head length using the Open Comet automated tool used for assessing the comet lengths. The comet head diameters for Co_3O_4 showed 0.5 mm and had no tail formations. Similarly, the test samples 1% having 50 and 150 µg/mL diluted concentrations had 0.5–0.7 mm head diameters expressed with no tail formations, whereas the 3% and 5% having different concentrations showed varying tail lengths from 1.1 to 1.3 mm, as shown in Table 2. This evidently confirms the DNA damage of the > 3% concentrations of Cr-doped Co_3O_4 nanoparticles against the genomic DNA chosen, as shown in Fig. 6 [28, 29].

In vitro anticancer activity of pure Co_3O_4 and Cr-doped Co_3O_4 NPs

The IC50 values for each concentration of nanoparticles were determined based on the cell viability rates. The morphological profiles of the cell culture plates viewed after 24 h and 48 h sample treatments

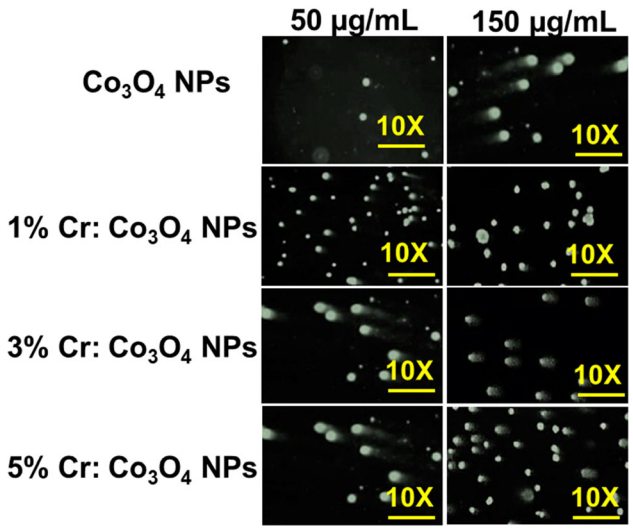

Figure 6 In vitro studies of DNA damage of pure Co_3O_4, 1% Cr: Co_3O_4, 3% Cr: Co_3O_4 and 5% Cr: Co_3O_4 nanoparticle.

under the inverted microscopes are given in Fig. 7. The IC_{50} observed for the test samples, pure Co_3O_4 and Cr-doped Co_3O_4 nanoparticles nanocomposite showed 29.43 ± 1.44, 43.22 ± 1.02, 56.93 ± 1.41, 60.68 ± 1.05, 40.02 ± 1.14, and 69.83 ± 1.33, respectively [29].

Conclusion

In summary, the 5% Cr-doped Co_3O_4 nanoparticles were prepared using the co-precipitation method, where the XRD and FESEM studies confirmed the formation of cubic phase and irregular spherical shape with the aggregated structure of Co_3O_4, 1% Cr: Co_3O_4, 3% Cr: Co_3O_4 and 5% Cr: Co_3O_4 nanoparticles, respectively. The grain sizes were 21.5, 23.5, 25.2 and 28.7 nm. The confirmed nanoparticles were then used to assess DNA damage using the hemolysis and comet assay. In addition, the cell viability assessments were carried out on *HeLa* cervical cancer cell lines. The outcomes suggest that the prepared nanoparticles were highly hemocompatible, showing inducible DNA damage via tail moments. The cell viability assays showed that the nanoparticles have detrimental effects on the cancer cells via morphological and MTT assay results. Therefore, the studied concentrations of 5% Cr-doped Co_3O_4 can be further used as an efficient hemocompatible and anticancer-based nanomaterial in future therapeutic aspects.

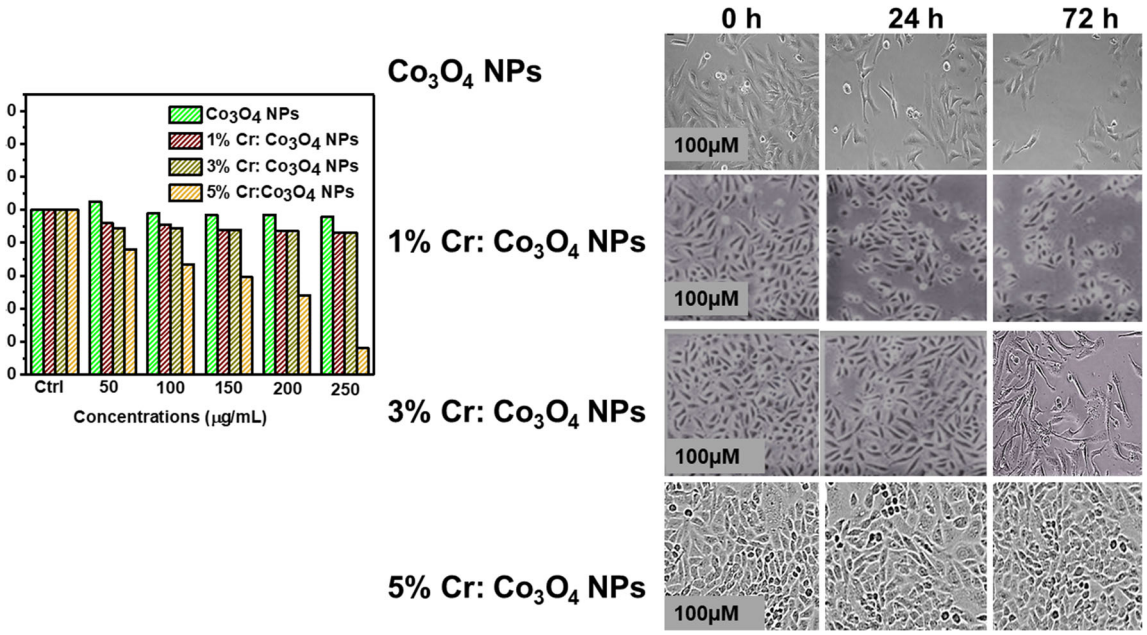

Figure 7 Bar diagram of cell viability of pure Co_3O_4 and 1, 3 & 5% Cr-doped Co_3O_4 NPs and morphology image of pure Co_3O_4 and 1, 3 & 5%Cr-doped Co_3O_4 NPs on HeLa cancer cell lines using optical microscopy.

Acknowledgements

The authors are grateful to DST-FIST and UGC SAP, New Delhi, India, for the instrumentation facilities.

Author contributions

SS: Conceptualization, Methodology, Data curation, Writing original draft, Investigation, Formal analysis. VM: Formal analysis. PPV: Conceptualization, Validation, Review & editing, Visualization, Supervision.

Funding

Funding was provided by the RUSA 2.0 - BEICH Government of India.

Declarations

Conflict of interest The authors declare no conflict of interest to the manuscript.

References

[1] Jadhav K, Deore S, Dhamecha D, Hr R, Jagwani S, Jalalpure S, Bohara R (2018) Phytosynthesis of silver nanoparticles: characterization, biocompatibility studies, and anticancer activity. ACS Biomater Sci Eng 4(3):892–899.

[2] Thorat ND, Bohara RA, Noor MR, Dhamecha D, Soulimane T, Tofail SA (2017) Effective cancer theranostics with polymer encapsulated superparamagnetic nanoparticles: combined effects of magnetic hyperthermia and controlled drug release. ACS Biomater Sci Eng 3(7):1332–1340.

[3] Mrue F, Netto JC, Ceneviva R, Lachat JJ, Thomazini JA, Tambelini H (2004) Evaluation of the biocompatibility of a new biomembrane. Mater Res 7(2):277–283.

[4] Cemeli E, Baumgartner A, Anderson D (2009) Antioxidants and the Comet assay. Mutation Res/Rev Mutation Res 681(1):51–67.

[5] Chattopadhyay S, Dash SK, Tripathy S, Das B, Mandal D, Pramanik P, Roy S (2015) Toxicity of cobalt oxide nanoparticles to normal cells; an in vitro and in vivo study. Chemico-Biol Interact 226:58–71.

[6] Iravani S, Varma RS (2020) Sustainable synthesis of cobalt and cobalt oxide nanoparticles and their catalytic and biomedical applications. Green Chem 22(9):2643–2661.

[7] Khan S, Ansari AA, Khan AA, Ahmad R, Al-Obaid O, Al-Kattan W (2015) In vitro evaluation of anticancer and antibacterial activities of cobalt oxide nanoparticles. JBIC J Biol Inorg Chem 20(8):1319–1326.

[8] Yu ZG, Yang BC (2008) Morphological investigation on cobalt oxide powder prepared by wet chemical method. Mater Lett 62(2):211–214.

[9] Bisht V, Rajeev KP (2011) Non-equilibrium effects in the magnetic behavior of Co3O4 nanoparticles. Solid State Commun 151(18):1275–1279.

[10] Sundar LS, Singh MK, Pereira AM, Sousa AC (2019) The cobalt oxide-based composite nanomaterial synthesis and its biomedical and engineering applications. In: Cobalt Compounds and Applications, Intech Open.

[11] Malefane ME (2020) Co3O4/Bi4O5I2/Bi5O7I C-scheme heterojunction for degradation of organic pollutants by light-emitting diode irradiation. ACS Omega 5(41):26829–26844.

[12] Vijayalakshmi K, Sivaraj D (2015) Enhanced antibacterial activity of Cr doped ZnO nanorods synthesized using microwave processing. RSC Adv 5(84):68461–68469.

[13] Khan SA, Shahid S, Bashir W, Kanwal S, Iqbal A (2017) Synthesis, characterization and evaluation of biological activities of manganese-doped zinc oxide nanoparticles. Trop J Pharm Res 16(10):2331–2339.

[14] Bandgar SS, Yadav HM, Shirguppikar SS, Shinde MA, Shejawal RV, Kolekar TV, Bamane SR (2017) Enhanced hemolytic biocompatibility of hydroxyapatite by chromium (Cr 3+) doping in hydroxyapatite nanoparticles synthesized by solution combustion method. J Korean Ceram Soc 54(2):158–166.

[15] Wadekar KF, Nemade KR, Waghuley SA (2017) Chemical synthesis of cobalt oxide (Co_3O_4) nanoparticles using Co-precipitation method. Res J Chem Sci 7(1):53–55.

[16] Vannier V, Schenk M, Kohse-Höinghaus K, Bahlawane N (2012) Preparation and characterisation of chromium-doped cobalt oxide spinel thin films. J Mater Sci 47(3):1348–1353.

[17] Ansari SM, Bhor RD, Pai KR, Mazumder S, Sen D, Kolekar YD, Ramana CV (2016) Size and chemistry-controlled cobalt-ferrite nanoparticles and their anti-proliferative effect against the MCF-7 breast cancer cells. ACS Biomater Sci Eng 2(12):2139–2152.

[18] Liu YK, Deng XX, Yang HL (2016) Cytotoxicity and genotoxicity in liver cells induced by cobalt nanoparticles and ions. Bone Joint Res 5(10):461–469.

[19] Sivaranjani S, Arya K, Ponpandian N, Vijaya PP (2021) Fabrication, toxicity and biocompatibility of Sesamum indicum infused graphene oxide nanofiber-a novel green composite method. Appl Nanosci 11(2):679–686.

[20] Farhadi S, Javanmard M, Nadri G (2016) Characterization of cobalt oxide nanoparticles prepared by the thermal decomposition. Acta ChimicaSlovenica 63(2):335–343.

[21] Sharma P, Sharma A (2016) Structural & magnetic properties of cobalt oxide nanoparticles at different annealing temperatures. Int J Mater Sci Eng 4:208–214.

[22] Reena RS, Aslinjensipriya A, Jose M, Das SJ (2020) Investigation on structural, optical and electrical nature of pure and Cr-incorporated cobalt oxide nanoparticles prepared via co-precipitation method for photocatalytic activity of methylene blue dye. J Mater Sci: Mater Electron 31(24):22057–22074.

[23] Hamadanian M, Sarabi AS, Mehra AM, Jabbari V (2014) Photocatalyst Cr-doped titanium oxide nanoparticles: fabrication, characterization, and investigation of the effect of doping on methyl orange dye degradation. Mater Sci Semicond Process 21:161–166.

[24] Nibret A, Yadav OP, Diaz I, Taddesse AM (2015) Cr-N co-doped ZnO nanoparticles: synthesis, characterization and photocatalytic activity for degradation of thymol blue. Bull Chem Soc Ethiop 29(2):247–258.

[25] Sarath Chandra V, Baskar G, Suganthi RV, Elayaraja K, AhymahJoshy MI, Sofi Beaula W, Narayana Kalkura S (2012) Blood compatibility of iron-doped nanosize hydroxyapatite and its drug release. ACS Appl Mater Interfaces 4(3):1200–1210.

[26] Uboldi C, Orsière T, Darolles C, Aloin V, Tassistro V, George I, Malard V (2015) Poorly soluble cobalt oxide particles trigger genotoxicity via multiple pathways. Part Fibre Toxicol 13(1):1–15.

[27] Nyga AT (2015) Mechanism of cobalt nanoparticle-induced cytotoxicity and inflammation in human macrophages

[28] Ajarem JS, Maodaa SN, Allam AA, Taher MM, Khalaf M (2021) Benign synthesis of cobalt oxide nanoparticles containing red algae extract: antioxidant, antimicrobial, anticancer, and anticoagulant activity. J Cluster Sci. 1–12.

[29] Mahalakshmi S, Hema N, Vijaya PP (2019). In vitro biocompatibility and antimicrobial activities of zinc oxide nanoparticles (ZnO NPs) prepared by chemical and green synthetic route—a comparative study. BioNanoScience. 1–10.